

Development of Implantable Light Source

BME 400

December 11th, 2019

Client: Dr. Matyas Sandor, Department of Pathology and Laboratory Medicine

Advisor: Dr. Justin Williams, Department of Biomedical Engineering

LEDMouse Team Members:

Ruochen Wang - Team Leader

Jacky Tian - BSAC/BPAG

Lisa Xiong - BWIG

Hanna Rainiero - Communicator

Abstract

Tuberculosis is a serious infectious disease with an increasing presence of antibiotic resistance further threatening populations. The Sandor lab is investigating immune cell trafficking as an alternative therapeutic target using photoconversion and optogenetic activation of immune cells utilizing photoactivation. KikGR mouse cells can be photoconverted from green to red when exposed to a 405 nm wavelength light and Ai32 mouse cells can be photoactivated when exposed to a 450-490 nm wavelength range. The current method for photoconversion/photoactivation involves a fiber optic cable with a needle attachment which lacks surface area exposure necessary for efficient photoconversion/activation. A previous semester design that utilized LEDs was improved with a printed circuit board (PCB). LEDs on a breakout board were used for ease of use, testing, and debugging. The LEDs successfully photoconverted KikGR mouse cells and was found to be within the photoactivation range of the Ai32 mouse cells. Temperature changes of LEDs stayed well below tissue coagulation temperatures over time. Overall, the team designed a safe, effective alternative to photoconvert and photoactivate immune cells which will aid the investigation of novel therapeutics for tuberculosis.

Table of Contents

Abstract	2
I. Introduction	5
II. Background	6
III. Competing Devices	7
IV. Previous Prototype	8
V. Biomaterial Selection	10
1. Parylene	10
2. Polydimethylsiloxane (PDMS)	10
3. MasterSil 151 Med	10
VI. Circuit Designs	10
1. Pin and Wire	10
2. PCB Integration	11
3. Implantable Connectors	11
Circuit Schematic	12
VII. Preliminary Design Evaluation	13
Permeability	14
Optical Clarity	14
Cost	15
Ease of Fabrication	15
Flexibility	15
Safety	16
Ease of Use	16
Stability	17
Ease of Fabrication	17
Cost	17
Proposed Final Design	17
VIII. Development Process	17
Materials	17
Circuit Schematics	18
Breakout Boards	19
Printed Circuit Board (PCB)	20

Code	23
Methods	23
Testing	23
IX. Results	25
X. Discussion	30
XI. Conclusions	31
XII. References	33
Appendix I: Product Design Specification (PDS)	37
Appendix II: Testing Result Calculation	40
Appendix III: Material Costs	40
Appendix IV: Arduino Code	40
Appendix V: MATLAB Code	46

I. Introduction

Tuberculosis (TB) is a serious infectious disease that is among the top 10 causes of death globally, and is the leading cause of death from a single infectious agent [1]. Drug-resistant TB is a public health crisis with over half a million individuals developing TB with resistance to rifampicin, the most effective first line drug, and of those resistant, 82% had multiple drug resistant TB [1]. This clearly indicates a need for novel therapeutics to treat TB. A pathological hallmark of TB is granulomas, immune cell clustering around sites of infection, which is a potential target for therapy. Continuous cell replacement has been demonstrated as a mechanism of immune trafficking to maintain the granuloma microenvironment surrounding TB, however further research is needed in this area [2][3].

Dr. Sandor and his lab members from the Department of Pathology & Laboratory Medicine, University of Wisconsin-Madison, are investigating continuous cell replacement to demonstrate plasticity of TB granulomas. They currently utilize two mouse models that express ion channels sensitive to light in their research: a KikGR33 mouse model which expresses green-red photoconvertible fluorescent protein at 405 nm and an Ai32 mouse model which expresses channelrhodopsins to allow photoactivation with exposed to 450 to 490 nm light (Fig. 1) [4]. Using a fiber optic cable, they illuminated small areas of affected tissue to photoconvert or photoactivate the cells. In KikGR mice, the lungs could then be excised up to seven days after photoconversion and examined to see the ratio of red immune cells that were photoconverted at the site to the green immune cells that were trafficked into the granuloma from unexposed tissue (Fig. 2) [2]. In Ai32 mice, calcium uptake by the cells can be observed to identify photoactivation.

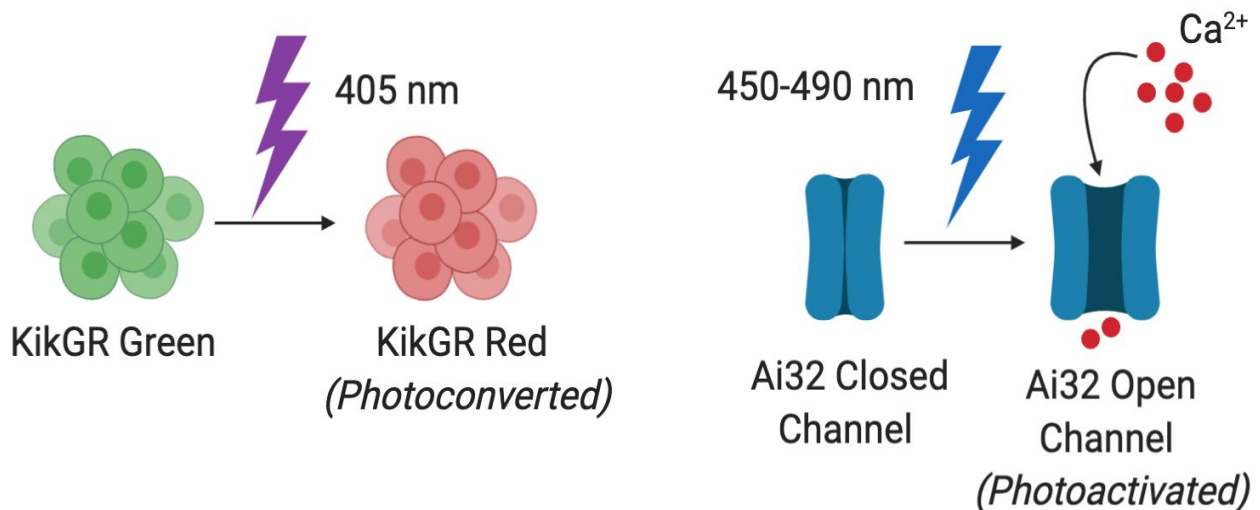


Figure 1. The Sandor Lab uses two mouse models: KikGR which has photoconvertible cells when exposed to 405 nm wavelength and Ai32 which has photoactivatable cells that undergo calcium influx by channelrhodopsins after exposure to 450-490 nm light (Biorender).

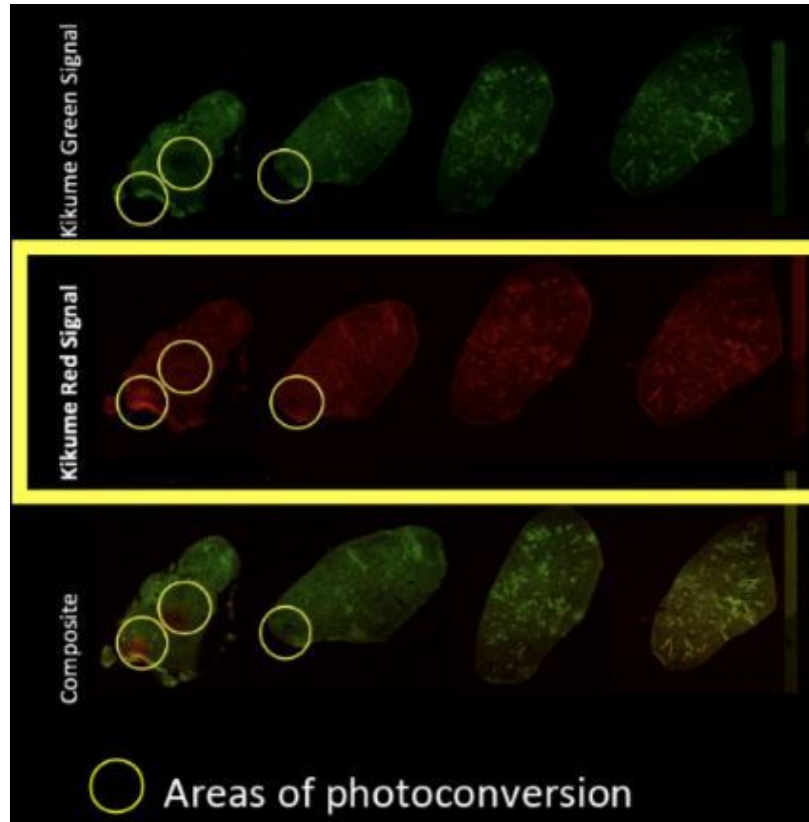


Figure 2: Photoconversion by fiber optic cable is limited. Pictured above is fluorescent signalling from the lungs of KikGR33 mice infected with TB that had sites photoconverted by the fiber optic cable used by Dr. Sandor and his lab. Note the small, inefficient area photoconverted (yellow circles).

A challenge to their research is inefficient photoconversion/photoactivation with their current method using a fiber optic cable. This semester our team designed and fabricated an implantable device and tested the photoconversion efficiency with KikGR33 mouse cells for Dr. Sandor and his lab’s tuberculosis research. Our device will mitigate the disadvantages of other current methods by being biocompatible, effective at photoconverting a larger area, and cheap to manufacture (See PDS Appendix I). Furthermore, our device will have implications for other research that utilizes optogenetics.

II. Background

The implantable LED device design areas include the light source for photoconversion/photoactivation, design of the LED circuit, and a safe, biocompatible coating for our final product. Our client, Dr. Sandor and his lab members, have given us requirements based off of their current research methods for photoconversion. A light strength of 95 mw/cm² light source has been cited as effective for photoconverting tissues [5][6]. Dr. Matyas has specified that an area of approximately 1 cm² is needed to illuminate the mouse lung. The

wavelength necessary for photoconversion of KikGR33 fluorescent protein used in the client's mouse model is 405 nm [4]. Another mouse model used is the Ai32 mouse that needs a 450 - 490 nm wavelength and 400 mW/cm² light strength to activate channelrhodopsins. Our client has requested that we develop a light source specific to the Ai32 mouse into a device as well. The light should limit photodamage and phototoxicity to the tissue. The implant should be biocompatible and must not trigger an immune response in the mouse (Appendix I).

The electronic design of our implant will require a power source such as a battery or an Arduino microcontroller, a board on which our LEDs are attached, and LEDs. The circuitry must be designed to provide the appropriate voltage and current for the LEDs. The LEDs themselves must have the appropriate wavelength emission of 405 nm for successful photoconversion and 450-490 nm for photoactivation. The electronics must not cause excessive heat within the mouse. The Association for the Advancement of Medical Instrumentation (AAMI) recommended that an implant should not increase the systemic body temperature by more than 1°C [7]. Additionally, tissue coagulation will occur between 50 °C and 60 °C, so the implant must remain well below that temperature threshold [8].

Considerations for our biomaterial include optical clarity, biocompatibility, and electronic inertness. Common biomaterials used to encapsulate medical devices that are optically clear include silicones and parylenes. Parylene C is the gold standard for encapsulating electronic devices due to its optical clarity, high dielectric constant, and low permeability to water and chemicals [9][10][11]. Medical grade silicones can also be used for encapsulating devices, however their biocompatibility is less ideal than Parylene C [12].

III. Competing Devices

There are devices available on the market for the photoconversion and photoactivation of KikGR33 and Ai32 mouse cells. Devices available on the market used for photoconversion documented in previous scientific studies are the USHIO SP500 and SP250 spot UV curing equipment and Leica Microsystems fluorescence stereo microscopes (Fig. 3) [5][6][13]. Prabhakar et. al [14] used a Fibertec II Fiber Coupled Diode Laser Module (Blue Sky Research) to photoactivate Ai32 mouse cells whereas Madisen et. al [15] used a 200-µm optical fiber coupled to a 593-nm yellow laser (Fig. 3). Although these devices may already be on the market, none of them utilize LEDs as a source of light, these current devices can be expensive and are not as convenient to operate as LEDs.

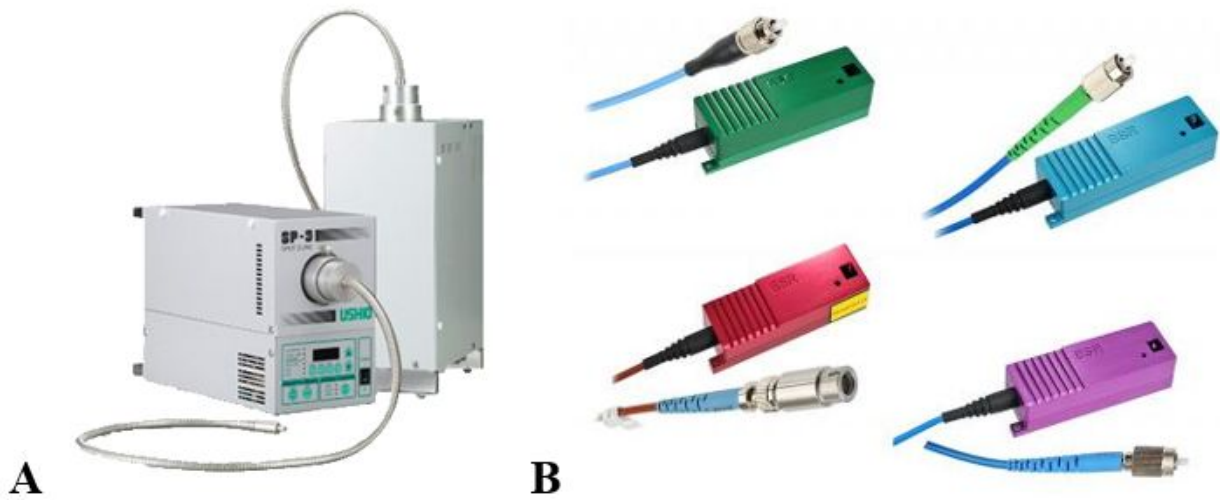


Figure 3: *A, The USHIO Spot-Cure Series, Spot UV Curing Equipment uses a low attenuation UV lamp [16]. B, Blue Sky Research's FiberTec II™ Series uses fiber-coupled lasers that incorporate modulation and feedback functions [17].*

IV. Previous Prototype

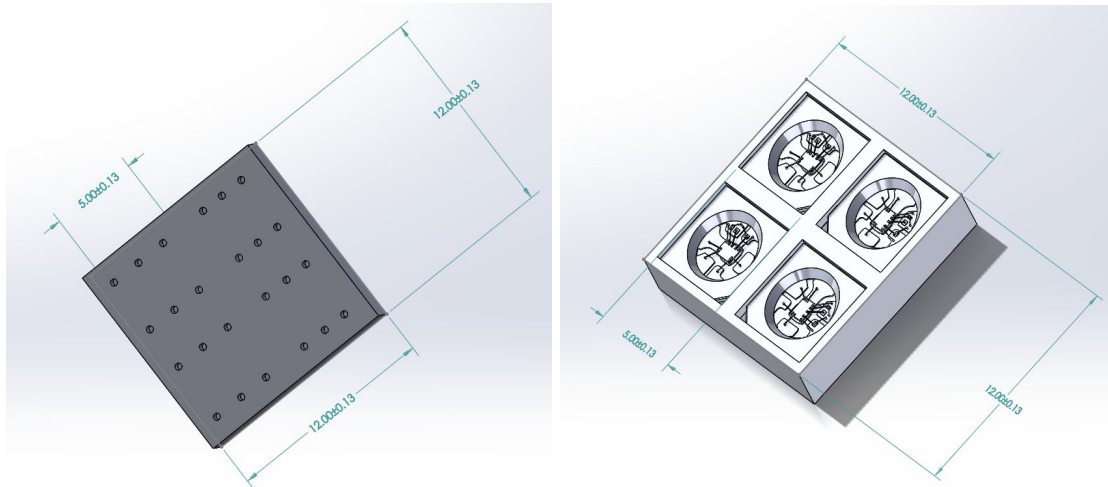


Figure 4: *Implementation of four LEDs in CAD.*

In BME 300, an LED mat design was developed (Fig. 4). In order to develop a light source that can deliver intense light to the region of interest in mice, we connected 4 LEDs together and placed it on a perf board that stabilized the LEDs. The idea of the previous design was to solder wires onto the pins of the LEDs and the other end of the wire would pass through the perf board holes.

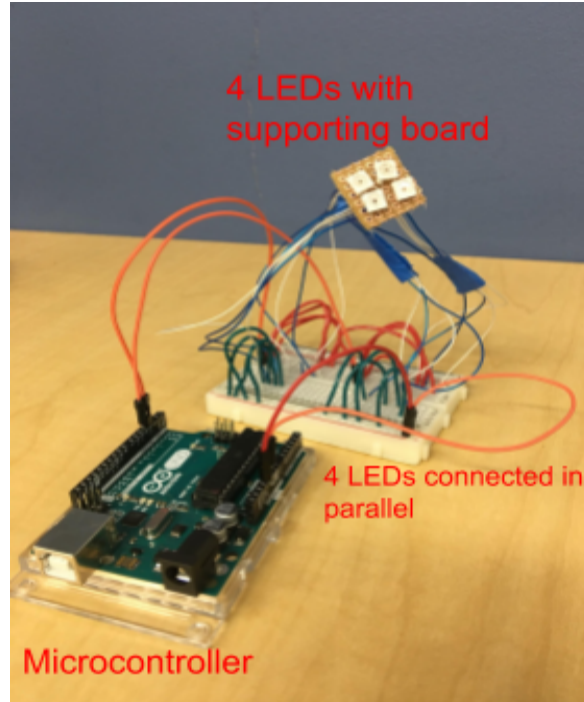


Figure 5: Fabricated prototype from BME 300 Fall 2018 semester.

The final prototype developed in BME 300 used an Arduino Uno, a breadboard, perfboard, wire connections and LEDs (Fig. 5). A code was developed in Arduino to send signals to the LEDs to control the brightness and wavelength. The microcontroller was powered by a USB-B connected to a laptop and could output 5V to the circuit. The four LEDs were connected in parallel by the circuit built on the breadboard. Each LED consists of 4 pins that serve different purposes. Pin 1, Data Input, was used for receiving instructions from the Arduino code. Pin 2 was Data Output, used for synchronizing the LEDs and allowing them to be linked in series. Pin 3 was to ground the LEDs, and pin 4 was the VCC+ pin that provided 5V from the microcontroller. Testing confirmed that last year's prototype could deliver 480 nm light.

The last step was to coat the device with a biocompatible material. The biomaterial chosen was polydimethylsiloxane (PDMS) which is widely used in biomedical implants due to its optical clarity, flexibility, and inertness [18][19]. We did not synthesize PDMS of our own last year because of the difficulty in manufacturing them. Instead, we attained PDMS scraps from McClean Lab in the Department of Biomedical Engineering and placed the already-solid form of the PDMS on top of the LEDs to test if the biomaterial would refract or attenuate light delivery.

The testing results showed that the prototype was effective: the tested light intensity of the device ($>800 \text{ mW/cm}^2$) was much higher than the requirement (95 mW/cm^2). Results from the spectrometer showed a peak wavelength at 480 nm, indicating the connections of LEDs, biomaterial coating, and coding on Arduino Uno were reasonable. However, one LED out of the four was not working throughout the testing process. The reason could be the LED was damaged

from the fabrication process and pin-and-wire connection problems. The small size of the LEDs and difficulty to accurately and securely solder the wires to the LED pins could have contributed to unstable connections. The wires would fall off from the pins easily when the devices were handled. In this semester, our team sought to refine the previous prototype by finding a better way to stabilize the LEDs and further test the effectiveness of our device.

V. Biomaterial Selection

1. Parylene

Parylene has become the gold standard for protective coating of implantable electronics, aerospace and medical applications and has a Young's Modulus of ~ 4 GPa [20]. Parylene is characterized as chemically and biologically inert, low water permeability and absorption, which are the preferred characteristics to our project. There are existing designs from research groups that utilizes Parylene C as encapsulation materials and substrate for intraocular pressure (IOP) monitor [20] and neural electrodes for recording [21].

2. Polydimethylsiloxane (PDMS)

PDMS is a material that has a Young's Modulus of 360-870 kPa [22]. The low Young's Modulus also contributes to its unique flexibility. It has strong dielectric strength, biocompatibility and low chemical reactivity. These properties made it a candidate for our encapsulating material of the device. Since it is flexible and high dielectric strength, it could be used for pressure sensing by changing its capacitance because of the pressure. Some other groups have also used the PDMS as the material for an IOP monitor [23]. It is light transparent in the visible region and highly absorbent at some wavelengths in the near infrared region.

3. MasterSil 151 Med

MasterSil 151 Med is a commercially available silicone substance that is engineered for use with electronics. It is biocompatible, optically clear, electrically insulative, highly flexible, and resistant to water. It has a bond shear strength of >50 psi, 800-900 psi tensile strength, and a service temperature range of -65 °F to $+400$ °F [24]. Since it is also transparent and has high refractive index, with its flexibility and biocompatibility, a group made contact lens for IOP monitoring with resonance circuit embedded in the material [25]. Furthermore, other groups have used it to encapsulate the printed circuit board (PCB) for intracranial pressure (ICP) [26].

VI. Circuit Designs

1. Pin and Wire

The pin and wire design was the final design in BME 300. The design has each tiny LED (5mm x 5mm) soldered with the thin wires to each pin respectively. The design then integrated 4 LEDs on top of an insulating board, and let their wires go through the holes in the perf board. The LEDs were stabilized on the board with glue and the biomaterial chosen would coat the device to make the design complete.

The design utilized common materials: thin wires and an insulating board with holes to address the problem. However, there were some difficulties during the fabrication process. The soldering was not stable and could easily come off during further fabrication, such as when integrating the LEDs on the board. Therefore the design was scored 2 and 3 for its safety and stability criteria. If the pin-wire connection was broken during the process, then the device is neither reliable nor safe for implantation into mice.

In the previous design, we chose LEDs with an adjustable wavelength to achieve the target wavelength (480 nm). There were 4 pins for each LED that were needed to be soldered. For each device, there were 4 LEDs on the board and a total of 16 wires were needed to be connected to power the device. The number of wires would be troublesome for both our client and the group as it would be harder to keep track of the wires. Therefore we rated the ease of use as 2 out of 5. If the client had no experience in electric circuits, the device could be connected to the wrong pins and the device would not function as desired.

The fabrication process was not optimized or streamlined for each device, the small pins were hard to solder to wires and gluing the LEDs on the board was difficult as well, so we gave the ease of fabrication criteria as 2 for this design.

2. PCB Integration

This design is an extension of the concept of placing the LEDs on a board with the last design. However, this design integrates the LEDs directly on the printed circuit board (PCB) with soldering, so that there is no glue needed for stabilizing the LEDs on the board. By printing the circuit on the board, we can also eliminate further wire usage since we are able to connect the pins of the LEDs to the PCB. Therefore, less wires will be required to connect the board, so we rated it 4 for safety and stability criteria; it will be less likely that the pins will fall off and less connections will be broken with less wires. We also rated this design 4 out of 5 for ease of use because the client would only need to connect one wire for each pin instead of 4 wires for each LED in the last design. This design would also be easier to fabricate because we could use a reflow oven available on campus for soldering. It would cost similar to the last design with more budget spent on materials and delivery.

3. Implantable Connectors

The Implantable Connectors design is an improved modification to the Pin and Wire design. Instead of having 16 wires extending from the LEDs, the wires would be consolidated

through a customizable, flexible, compatible, and implantable substrate. The implantable connector would be attached to a secure compartment which would contain the electronics to power the LEDs. Although these connectors are suited for the environment our LEDs will be operating in, it scored second highest because of the cost and ease of fabrication. The team would need to spend money to purchase the correct materials for the implantable connectors, and the fabrication would be difficult since the resources to create the connections on the flexible may require advanced machines. It would be challenging to build connections on a thin substrate layer.

Circuit Schematic

The Pin and Wire, PCB integration, and Implantable Connectors are different design ideas the team came up with to connect multiple wires to the LEDs. Each design will work with the improved circuit schematic that will make the LED connections more efficient. The LEDs will be connected in parallel to the power input and ground to allow all the LEDs to receive the same amount of voltage. We are not concerned with light intensity decreasing because the previous prototype reached an intensity at least eight times the required intensity. The datasheet for one of the LEDs used in this project has a schematic of a common setup for the LEDs. The team plans to connect the “digital in” pins (Din) of four LEDs in series (Fig. 6 and 7).

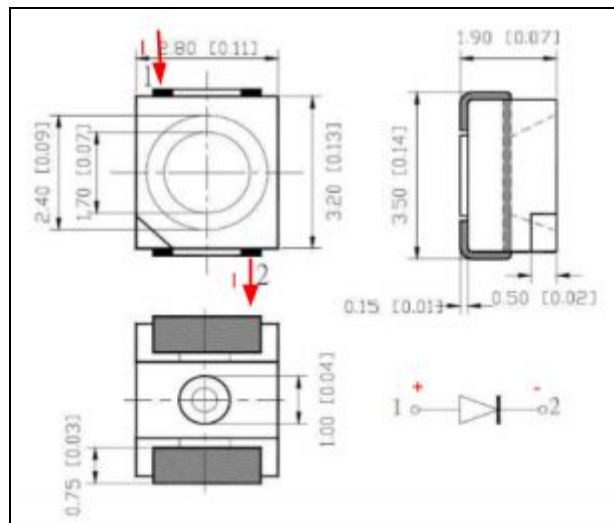


Figure 6: The LED for the 405nm wavelength is a two pin diode. Current will flow into pin 1 and out pin 2, continuing onto the next LED [27].

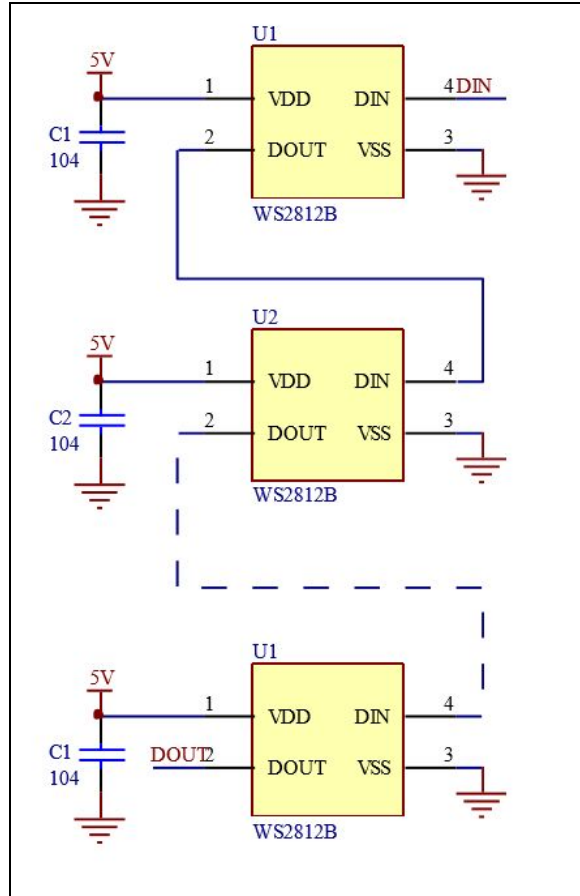
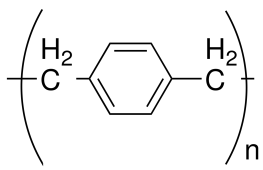
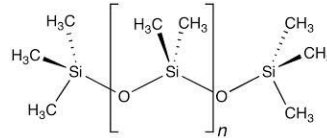



Figure 7: The LED for the 480nm wavelength is a 4 pin diode. The diodes are connected in series via the Din and Dout pins, which allow us to control the voltage input and wavelength output with the use of a microcontroller [28].

VII. Preliminary Design Evaluation

Table 1: Design Matrix for Biocompatible Coating

Criteria (weight)	Parylene 	PDMS 	Mastersil 151 Med 
Biocompatibility (40)	5/5	3/5	4/5
Ease of Fabrication (25)	3/5	4/5	5/5

Permeability (13)	5/5	2/5	4/5
Optical Clarity (10)	5/5	4/5	4/5
Flexibility (7)	3/5	4/5	5/5
Cost (5)	5/5*	5/5*	4/5
Total (100)	87.2	67.8	86.4

*available with campus resources

Safety (Biocompatibility)

Safety was defined as the “biocompatible rating” of the material. Since the light emitting diodes would be implanted into the mouse for a maximum of two hours, the biocompatible materials must be able to protect the electronic components and repel the organic fluids. The material also must not trigger inflammation or an immune reaction within the mouse.

Safety was ranked as the second most important criteria with a weighting of 20%, because we need to keep the mouse alive and with little inflammation to ensure the data our client collects is reliable. We decided that the material with the most biocompatibility was parylene because it is FDA approved for implantation in the body and has low permeability to water and is both chemically and biologically inert [18]. While medical grade silicone and PDMS have similarities with parylene, they lack the extremely low permeability to water that parylene offers which ensures the device will not harm the mice and the electronics will be safely isolated from the bodily fluids. Parylene C is considered the gold standard for devices implanted that need to resist both moisture and chemicals [9].

Permeability

Permeability was defined as the extent to which the material resists absorbing water and/or chemicals. We need an effective barrier that will not allow chemicals or water to damage the electronic circuits. Due to its implications with integrity and longevity of the device, we rated Permeability at 15%--tied for the third most important criteria for our device. Parylene had the highest score due to its very low permeability to water and chemicals while medical grade silicone and PDMS are susceptible to chemicals and water permeating through the material. This would put the electronics within the implant at risk of damage.

Optical Clarity

Optical clarity was defined as the effect of the coating on the wavelength or strength of the light emitted from the diodes. Parylene C was rated highest due to its thin film compared to PDMS and the Master Sil 151 Med. Parylene C is applied via vapor deposition, allowing the

biocompatible coating to be very thin. In comparison to PDMS and Master Sil, both require the electronics to be “dipped” which can create a thick coating. Parylene C’s method of application also allows the coating to be uniform which would decrease the change and refraction of the wavelength from the light emitting diodes [29].

Cost

Cost was ranked as the lowest criterion (5%) because we had some freedom to use our budget as needed provided by our client. In addition, it is possible to synthesize the biomaterials we need in labs here at UW-Madison, potentially at low costs. Therefore, our team considers cost to be a less critical factor in our design evaluation.

Ease of Fabrication

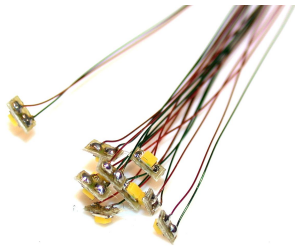
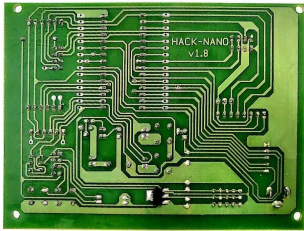
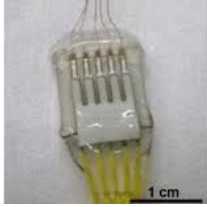
Ease of fabrication was an important factor with a weight of 25% in our design evaluation. To choose the proper biocompatible material for coating our device, our team needed to consider whether we could manufacture the material, or through online purchase, in this semester with the sources our team can acquire. Our team had experience in fabricating and using PDMS, so our team agreed that PDMS would be easy to fabricate. Also, the team found labs on campus that could manufacture PDMS. For the medical grade silicone, our team did research on different forms of silicone in manufacturing and found that the liquid injection might be a promising and manageable method for our project. Therefore, our team gave a 4 out of 5 to PDMS in terms of ease of fabrication. For the parylene, our team should do more research on the fabrication method of parylene and whether parylene can be manufactured following procedures our team can actively participate in. Therefore, for the unknown characteristics of this material, our team gives 3/5 to parylene. We ranked MasterSil 151 Med the highest because it is a manufactured and readily purchasable material that would not require curing or advanced machines like PDMS and parylene.

Flexibility

Since our device would be implanted into mice and our client wanted our device to be flexible to deliver light to different regions for a period of time, the biomaterial our team choose should also have the flexibility to meet this criteria. PDMS has high flexibility, which is why we have it a 5 out 5 to the medical grade silicone [22]. Since PDMS is vapor deposited, it may not be as flexible as PDMS. The MasterSil Med may not be as easy to manipulate as the PDMS. Therefore, our team assigned lower scores to PDMS and parylene [24][29].

Table 2: Design Matrix for Electronic Circuit Design

Criteria (weight)	Pin and wire	PCB integration	Implantable connectors
--------------------------	---------------------	------------------------	-------------------------------

			
Safety (30)	3/5	4/5	5/5
Ease of Use (30)	2/5	4/5	2/5
Stability (20)	2/5	5/5	4/5
Ease of Fabrication (15)	2/5	4/5	3/5
Cost(5)	5/5	4/5	3/5
Total (100)	49	84	70

Safety

Safety was ranked as the most important criteria with a weight of 30% because we need to protect the mouse from the electricity powering our LEDs and prevent the mouse blood from seeping into the electronics. The pin and wire design was ranked the lowest because of the 16 wires that would be needed to operate the LED. These 16 wires would have current running through them which could potentially be fatal to the mouse. Improving its safety would require coating the wires or covering them with protective plastic which will increase the time needed to fabricate the LEDs. The PCB board is ranked next highest because it will consolidate and simplify the wires connected to the LEDs. The LEDs would be powered via the PCB board, but still required power wires to be insulated. The implantable connector is rated highest because they are designed to be operable in *in vivo* environments. Implantable connectors utilize a biocompatible and secured container which houses the electronics.

Ease of Use

Ease of use was ranked second with a weight of 30% because we need to make sure our design would be simple and easy to use for our clients. Our clients do not have any electrical engineering background, and ideally, they could activate the LED and program code using a microcontroller. The pin and wire was ranked one of the lowest because we were concerned the wires would complicate the connections to and from the microcontroller. The implantable connectors were also ranked low, since more complex designs would require more work to connect the LEDs and make them functional. The PCB board was ranked highest because we

could power multiple LEDs with the PCB board, consolidate the number of wires, and decrease user confusion.

Stability

Stability was ranked third with a weight of 20% because we needed to consider how much movement will be involved once it is in the mouse. The pin and wires were ranked the lowest because the sixteen wires would cause more movement in the mouse. The implantable connectors are ranked the second highest because they would apply differently in the head compared to the chest cavity. The PCB board was the most stable because it will have the LEDs wired on a single entity, which reduces the movement inside of the mouse.

Ease of Fabrication

Ease of fabrication was the second to last to consider since we had many electric circuit fabrication methods and biomaterial fabrication techniques available both on campus and online. Therefore, the ease of fabrication was less of consideration for the design matrix. The PCB board scored the highest in this criterion because it could be designed through computer software and then be fabricated either at the Makerspace or sent to a company to produce for us. The benefit of the PCB board is that it can be mass produced for future use in case our client would need more LED devices.

Cost

Cost was ranked the least with a weight of 5% because the criterion for device's performance was more important than the cost. Moreover, for our current design, the most expensive material was the biocompatible coating. Our client also does not have a budget limit on the materials that we need to purchase. We expect our prototype to cost less than \$1,000 and the materials used in the design will be well below our cost threshold.

Proposed Final Design

The proposed final design the team will move forward with is the PCB integration with the use of Parylene C as the biocompatible coating.

VIII. Development Process

Materials

LEDs are an essential part of our project since we are making an implantable light source. The LEDs we are considering are Luxeon LEDs and a small OLED display. The Luxeon LED is very small and has multiple colors which produce different wavelengths, which our client wants on our implantable light. The small OLED display is a thin strip of lights, which would work well in exposing the maximum amount of lung cells to the light source. In addition, biomaterials

are key in our design as well because the light is being implanted into the mice, so it must not cause a reaction in the mouse. For the base of our structure a bioinert metal such as stainless steel or titanium could be used [21]. The light source will need to be covered by a transparent biomaterial such as Polydimethylsiloxane (PDMS) [22].

Small Luxeon lights of 405 nm wavelength and 480 nm wavelength will be connected via a PCB board and incorporated into a biocompatible and flexible material. The LEDs will protrude the board slightly and will be covered by biocompatible material. This will allow the light to be enclosed from the internal environment of the mouse while still allowing for light to pass through. The LEDs will be powered and controlled by a microcontroller (ESP8266 NodeMCU). After the microcontroller is programmed, it will be able to command the LEDs to output the correct brightness and wavelength.

Circuit Schematics

480 nm LEDs - LED pin schematic and circuit schematic

The 480 nm LED is a 4 pin RGB pixel LED containing a smart circuit. This allows the LED to communicate with a microcontroller to output specific wavelengths and brightness. The LED has four pins and requires a 5V power input, a ground connection, a digital input pin to communicate to the microcontroller, and an output pin that can send the same microcontroller command to other 480 nm LEDs (Fig. 8).

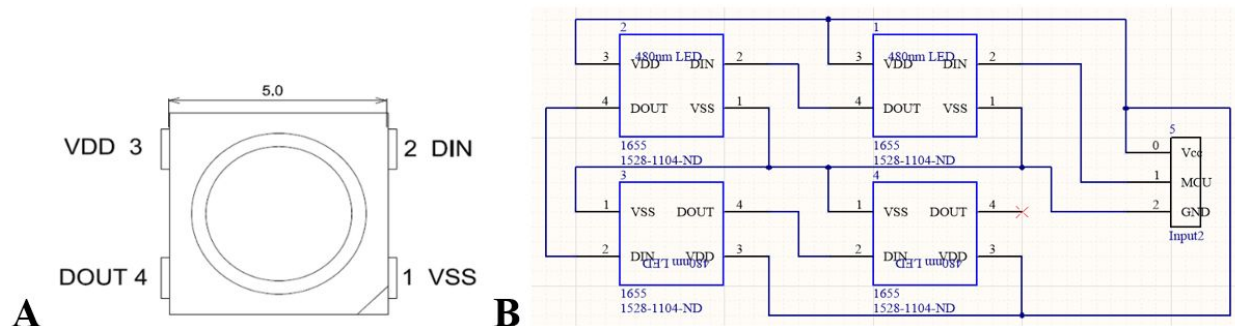


Figure 8: *A*, The 480 nm LED is a 4 pin device. Pin 1 (VSS) is the ground pin, pin 2 (DIN) is the digital input pin that communicates with the microcontroller, pin 3 (VDD) is the power pin where +5 V is input, and pin 4 (DOUT) is the digital output pin where the LED can send the signal it receives from the microcontroller to other LEDs [28]. *B*, The 480 nm LEDs were powered in parallel (+5 V) through the Vcc pin of the microcontroller (represented by the Input2 symbol), connected to ground through the GND pin of the microcontroller, and the LED designator 1 communicated to the microcontroller (pin 2 LED to pin 1 of Input2).

405 nm LEDs - LED pin schematic and circuit schematic

The 405 nm LED is a 2 pin device that is powered with 0-5 V and ground. Unlike the 480 nm LED, it is not wavelength variable; it only emits a 405 nm wavelength. The brightness of the LED can be changed by increasing or decreasing the voltage input (Fig. 9).

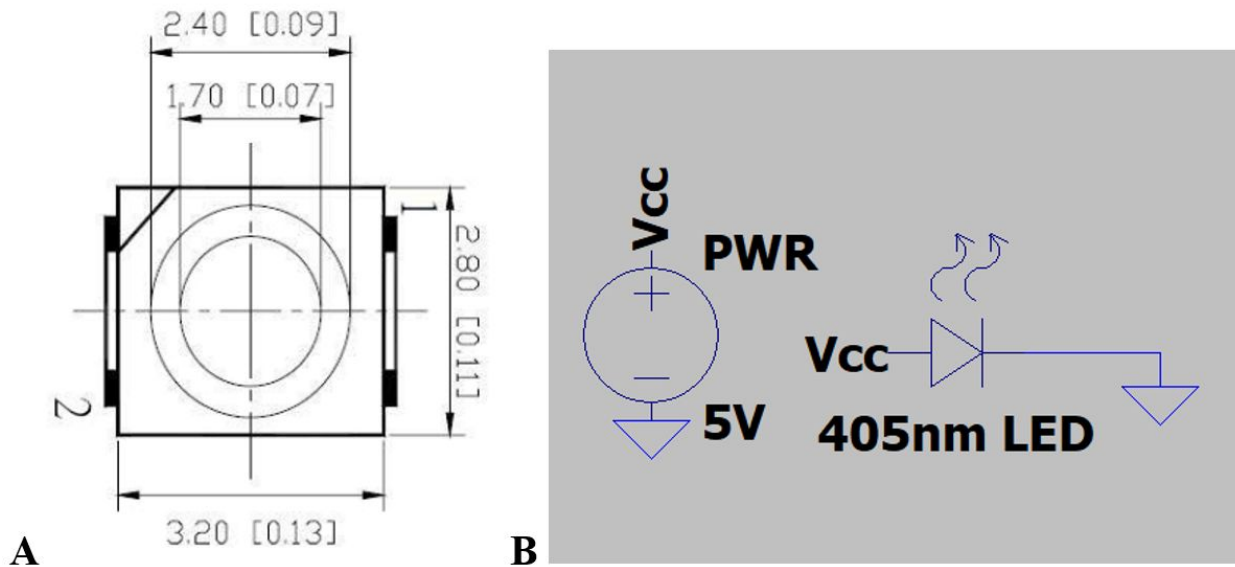


Figure 9: *A*, The 405 nm LED is a 2 pin device, powered with 0-5 V (pin 1) and connected to ground (pin 2, units in mm) [27]. *B*, LTSpice was used to create the circuit schematic. The PWR symbol represents a power supply of +5 V which is input into pin 1 of the LED represented by the triangle-vertical line symbol. It is then connected to ground.

Breakout Boards

Both the 480 nm and 405 nm LEDs were soldered onto a breakout board for ease of use, debugging with code, and to prototype connections to help finalize the PCB design. A manufactured breakout board with SMD footprints was ordered to solder the LEDs onto it along with header pins to connect to a breadboard (Fig. 10) [30].

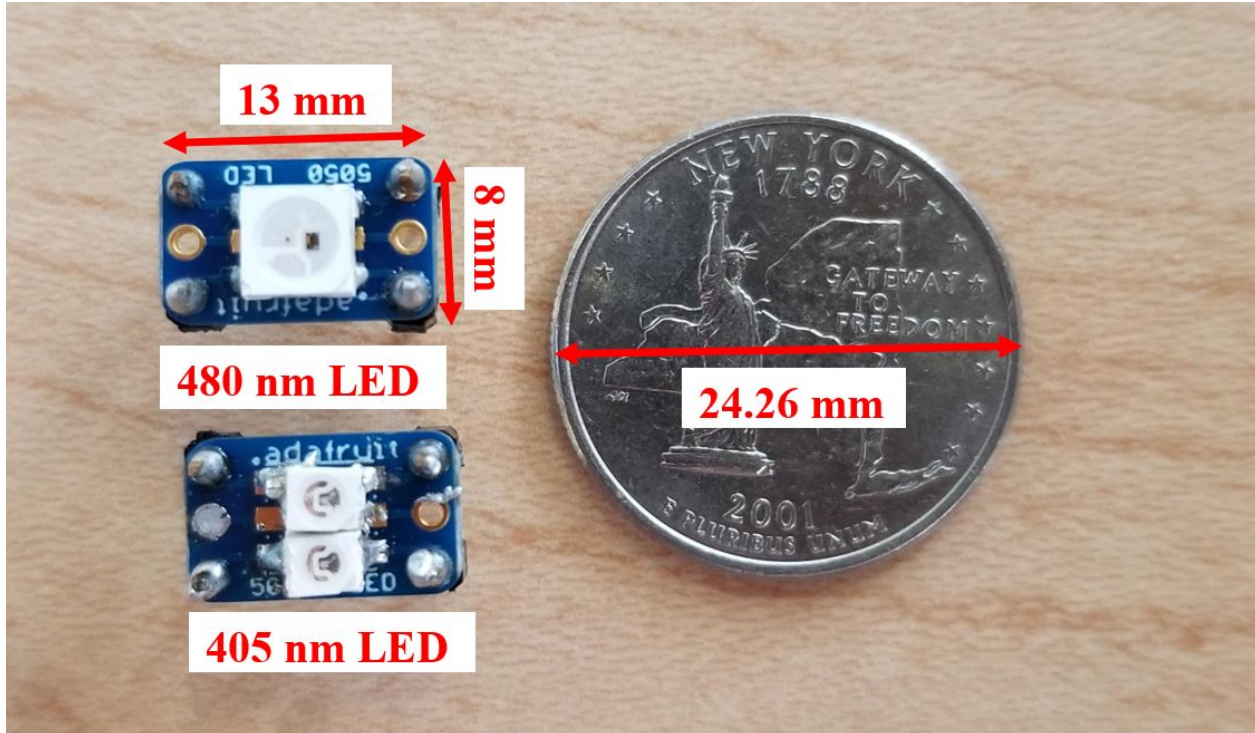
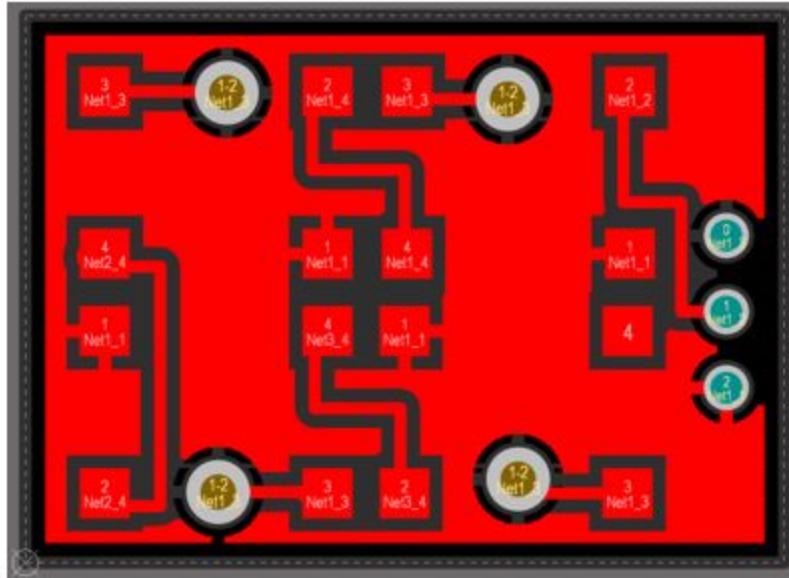


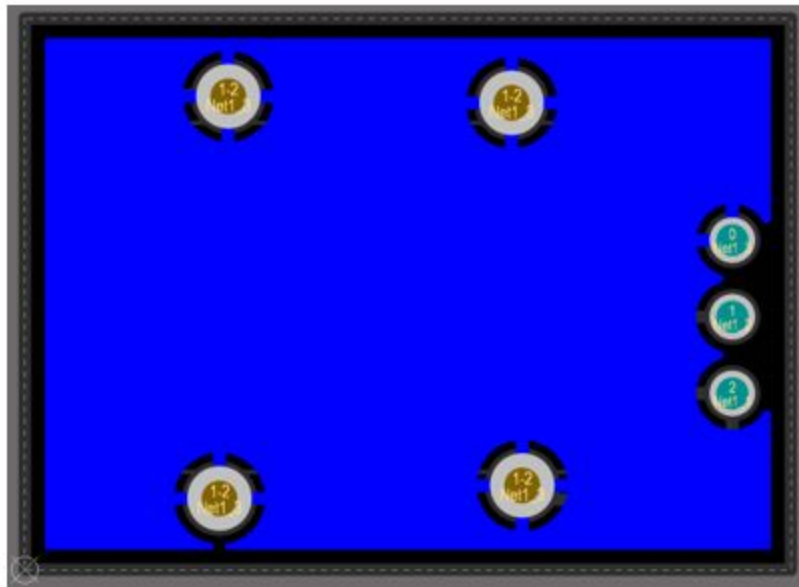
Figure 10: The 480 nm LED and 405 nm LEDs are soldered onto a breakout board and are compared to a quarter to show the size difference.

Printed Circuit Board (PCB)

The PCB was designed using *Altium Designer*, an electronic design automation software package for designing PCBs. The PCB was designed using three through hole connections, and two polygon pours (Fig. 11). The through holes allowed power, ground, and communication with the LEDs using the microcontroller. Layers of power and ground using polygon pours were created so that it would connect to the pins of the LEDs via SMD connections. The ideal dimensions of the final PCB were 10 mm x 10 mm x 1mm (L x W x H) and the final dimensions were 13.3 mm x 9.65 mm x 1 mm (Fig. 12).



A



B

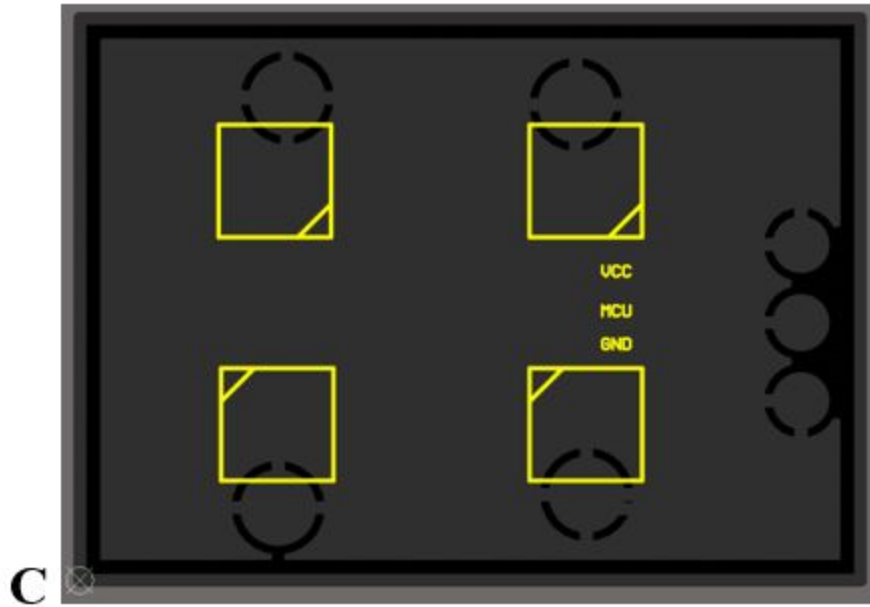


Figure 11: *A, The first polygon pour connects pins on the top layer to ground (represented as Net1_1). B, The second polygon pour connects pins from the top to the bottom layer to power (represented as Net1_3). C, The top overlay is the silkscreen layer, it does not have any electrical connections and is used to protect the user from the electrical layers of the PCB board. The drawings on these layers help orient the LEDs onto the PCB.*

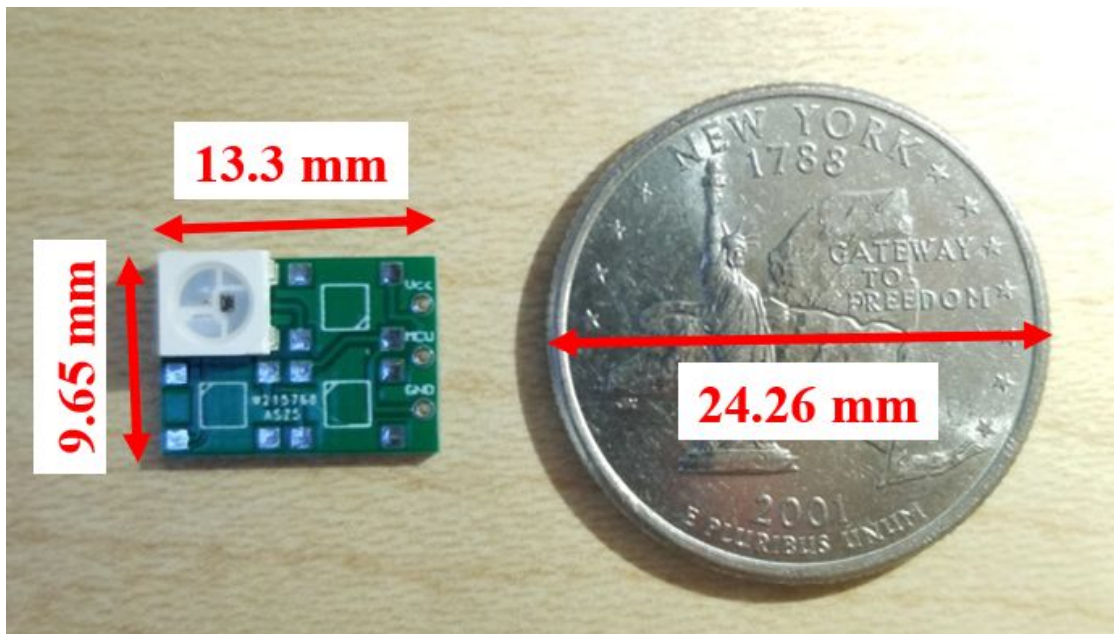


Figure 12: *The final PCB was fabricated through PCBWay and is compared to the size of a quarter.*

Code

Code was developed on Arduino to allow users of the 480 nm LED to change the wavelength, brightness, and pulse width modulation using the serial monitor (Appendix IV Fig. 19). Within the code there is a wavelength to RGB conversion; however, the Neopixel only can simulate the appearance of a color with three different wavelengths: red, green, and blue. As a result, the wavelength used must rely solely on the blue pixel of the Neopixel and the code is currently being used to control the brightness and pulse width modulation of the blue pixel within the Neopixel. An advantage of incorporating pulse width modulation is that the LED will emit light at frequencies close to which the channelrhodopsins fire so that the channels are not exposed during their refractory period before they can fire again. The pulse width modulation will also conserve more energy since it is not powered constantly and will reduce phototoxicity.

Methods

We calculated the mean and standard deviation and error for the wavelength and intensity testing because we were interested in the LED's wavelength range output and maximum intensity. For temperature testing, we performed a linear regression analysis to observe if there was a statistical significance in the relationship between change in temperature and time. Finally, we exposed KikGR33 mouse cells in 1.7 mL clear, conical tubes with 405 nm light to test for the LEDs' ability to photoconvert the cells *in vitro* for 0/5/15 minutes. The cells, after photoconversion, were dyed with trypan blue to evaluate cell viability. A two-way ANOVA test was performed to test for significance in cell fluorescence intensity after photoconversion in the different time durations.

Testing

Wavelength and Intensity Testing

For wavelength and temperature testing an Ocean Optics Spectrophotometer (USB2000+) was used to collect wavelength and intensity data from the LEDs. In order to minimize saturation of the spectrophotometer, the LEDs were kept at a distance of 12 mm from the spectrophotometer (Fig. 13). Wavelength and intensity data was collected in triplicates to identify the consistency of the LEDs with standard error calculations and to identify the mean wavelength range and mean peak within the required intensity range for each of the LEDs (Fig.16).

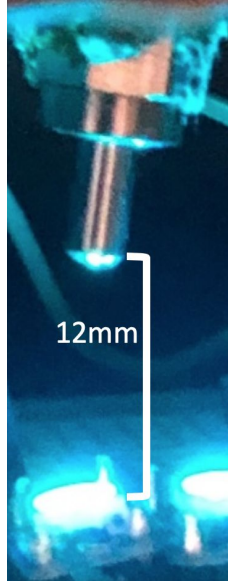


Figure 13: Intensity and wavelength testing of the LEDs. The wavelength and intensity were measured using an Ocean Optics Spectrophotometer (USB2000+) generously lent to us by the UW Madison biomedical engineering department. The LEDs were placed in a dark environment 12 mm away from the sensor to minimize saturation of the spectrophotometer.

Temperature Testing

For temperature testing of the LEDs to ensure that they were safe for *in vivo* studies, the temperature on the back of the breakout board of which the LEDs were soldered to was collected using an infrared laser temperature gun at 30 second intervals for a period of 5 minutes to recapitulate the actual time of the animal studies that the Sandor Lab will be using (Fig. 14) [2]. Regression statistics were performed to identify the relationship and variation of temperature of the LEDs over time. Additionally, the temperature was assessed to ensure it lies well below the temperature thresholds (See Appendix X for a more thorough protocol).

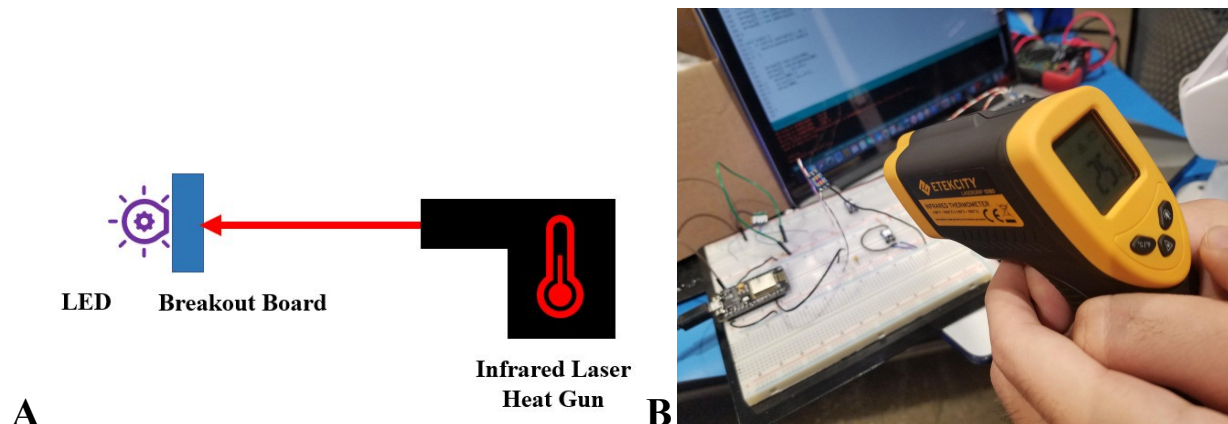


Figure 14: A-B, The temperature at the bottom of the breakout board was measured using an infrared laser heat gun.

In vitro testing

For *in vitro testing*, the LED device was brought to the Sandor Lab to test the efficacy of the 405 nm LEDs in photoconverting KikGR mouse lymph node cells. A cell suspension of lymph node cells from KikGR mice was pelleted in a 1.7 mL clear, conical tube. The tube was placed on top of the 405 nm LED for 5 and 15 min with a 0 min exposure control (Fig. 15). After exposure, the cells were resuspended, pipetted into a slide counter, and imaged under a confocal microscope. With no exposure to 405 nm wavelength light, the Kikume protein emits 517 wavelength light (green) under a fluorescent microscope when excited by a green laser (488 nm). With exposure of a 405 nm wavelength, the Kikume protein should undergo a conformational change and emit red (593 nm) when visualized under a fluorescent microscope after excitation with a red laser (594 nm). Cell viability was also assessed using Trypan blue following ~30 minutes after LED exposure.



Figure 15: *In vitro testing of KikGR cells with 405 nm LED. A lymph node cell suspension of KikGR cells was pelleted in a 1.7 mL clear, conical tube and placed directly on the 405 nm LED for 5 and 15 minutes with a 0 min exposure control (no exposure).*

IX. Results

Wavelength and Intensity results

For the LED intensity and wavelength testing, the data had to be further analyzed because the USB 2000+ gives a light intensity measured in counts every 100ms, and for our purposes intensity should be in units of mW/cm². Every count of photon energy is calculated with $h * c / \lambda$ where h is Planck's constant, c is the velocity of light, and λ is the wavelength measured (Equation 1). Since the counts are measured within 100ms, the number of counts in one second is 10 times more than the counts in 100 ms. The USB2000+ has light sensitive array

with 2048 pixels which is $14\mu\text{m} \times 200\mu\text{m}$ [6]. Then, the light intensity within a certain area may be calculated by the light energy divided by the pixel area (Equation 2).

$$E = \text{counts} * \frac{1\text{s}}{100\text{ms}} * \frac{h * c}{\lambda} \quad \text{Equation (1)}$$

$$\text{light intensity per area} = \frac{E}{\text{Area}} \quad \text{Equation (2)}$$

By using these 2 equations, the spectrophotometer intensity data could be converted into the light intensity units specified by the client. The data was then analyzed for mean wavelength and the upper and lower bounds of photoconversion or photoactivation, mean wavelength at peak intensity, and the standard error at each to compare consistency across the LEDs (Fig. 16).

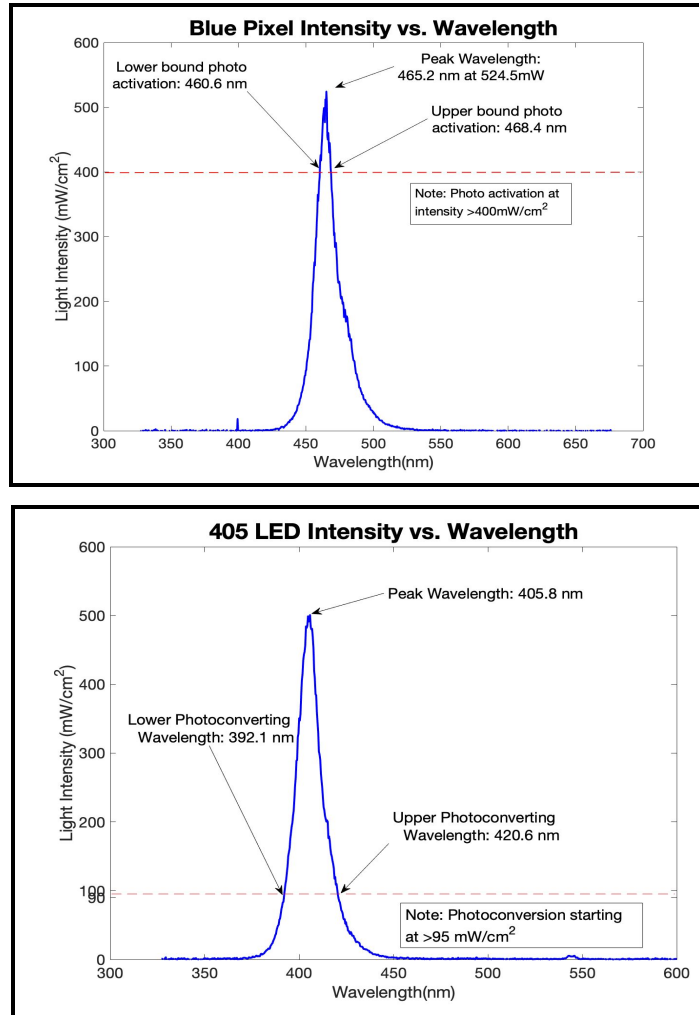
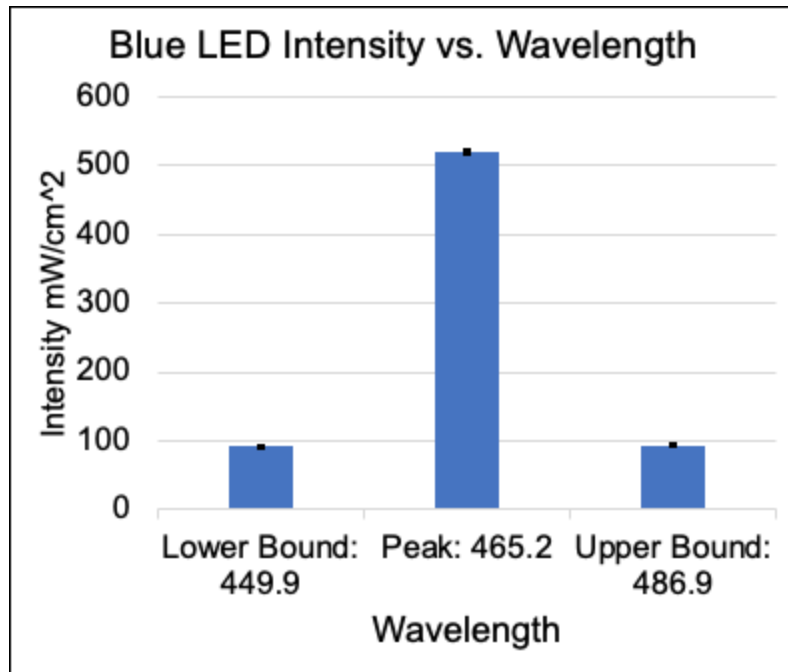
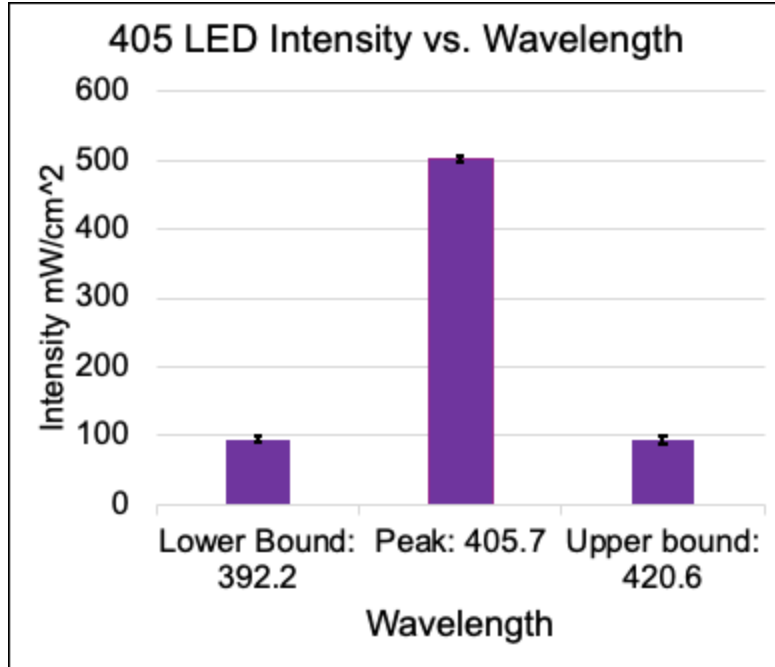


Figure 16: Wavelength vs. Intensity plots for the Neopixel (Blue Pixel) and 405 LED. The plots were analyzed using MATLAB (see Appendix V) to identify the standard error of the LEDs to ensure their consistency. Additionally, for the purposes of photoactivation and photoconversion, the mean LED wavelengths at the photoconversion upper and lower thresholds (95 mW/cm^2 for 405nm and 400 mW/cm^2 for 450-490 nm). Also the mean peak intensity and wavelength was assessed.

For the Blue LEDs, the mean lower bound wavelength at 400 mW/cm² was 449.9 nm (SE=4.02x10⁻¹⁴ nm) and the mean upper bound wavelength was 486.9 nm (SE = 0.1 nm). The peak wavelength and intensity was 465.2 nm (SE= 0 nm) and 520.73 mW/cm² (SE = 2.46 mW/cm²) (Fig. 17A). For the 405 nm LEDs, the mean lower bound wavelength at 95 mW/cm² was 392.2 nm (SE=0.1 nm) and the mean upper bound wavelength was 420.6 nm (SE = 6.96x10⁻¹⁴ nm). The peak wavelength and intensity was 405.7 nm (SE= 0.1 nm) and 501.9 mW/cm² (SE = 1.75 mW/cm²) (Fig. 17B).



A



B

Figure 17: *A. Wavelength vs Intensity within the photoactivating and photoconverting intensity threshold. The Blue LED photoactivating range (400 mW/cm²) is on average from 449.9 nm and 486.9 nm with a peak wavelength at 465.2 nm and intensity of 520.73 mW/cm². B. The photoconvertible range (95mW/cm²) of the 405 nm LED is on average from 392.2 nm and 420.6 nm with a peak wavelength at 405.8 nm and intensity of 501.9 mW/cm².*

LED temperature testing results

The results of the temperature testing on both the 405 nm and Blue LED revealed that the change in temperature is neither statistically significant nor correlated to time (regression analysis, p=0.565 and p=0.187). Additionally, the temperature was well below the threshold of 50 °C at which tissue will coagulate with the peak 405 nm temperature at 24.3 °C and the peak Blue LED temperature at 23.2 °C (Fig. 18).

Temperature Change of LEDs Over Time

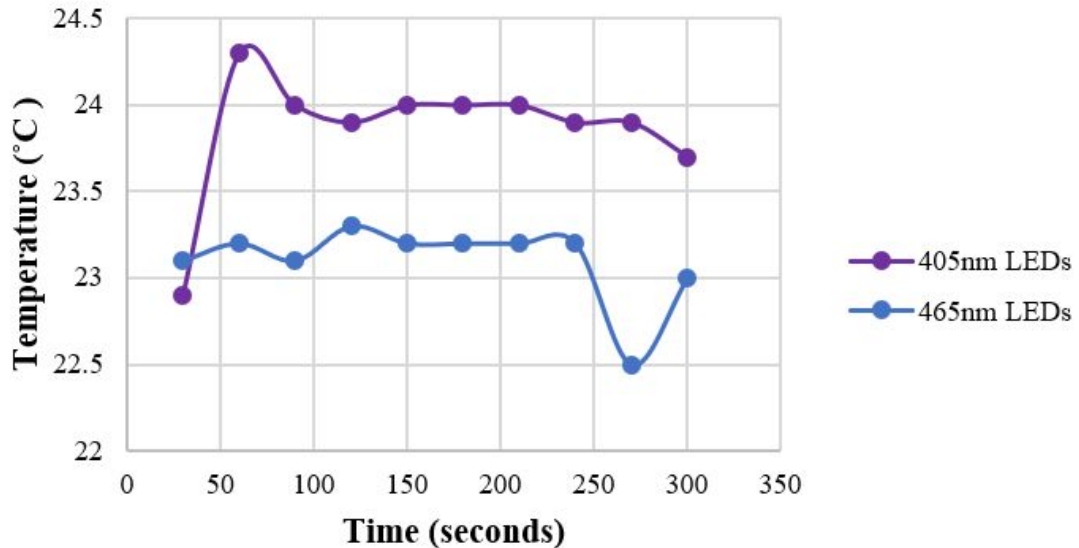


Figure 18: The temperature of the 405 nm and 465 nm LEDs over time is neither statistically significant nor correlated to time ($p=0.565$ and $p=0.187$). The LEDs maintained a safe working temperature well below the specification of below 50 °C.

In vitro testing results

To assess the efficacy of photoconversion by the 405 nm LED in KikGR cells, the mean fluorescence intensity in arbitrary units (AU) was measured for 100 cells at 0 min exposure (control), 5 min exposure, and 15 minute exposure (Fig. 19A). Successful photoconversion was observed with 5 and 15 min exposure photoconverting the cells from green to red (Fig. 19B). The mean intensity of the 0 min exposure was on average 18.84 AU for KikGR green and 7.10 AU for KikGR red (standard deviation (std) = 4.92, standard error of the mean (SEM)=0.492 and std = 0.37, SEM=0.037 respectively). In contrast, the exposed cells at 5 and 15 minutes showed on average 7.2 AU and 6.3 AU for KikGR green (std=0.57, SEM=0.057 and std=0.623 and SEM=0.06 respectively) and 22.98 AU and 22.49 AU for KikGR red (std = 4.85, SEM=0.485 and std=2.79, SEM=0.279 respectively) (Fig. 19C). In a two-way ANOVA the 5 and 15 minute exposure groups were significantly different from the 0 min exposure control ($p<0.0001$). There was no statistically significant difference between the 5 minute and 15 minute exposure group. Cell viability assessed with trypan blue was shown to be unaffected between experimental groups shortly after exposure to the LEDs (Fig. 19D).

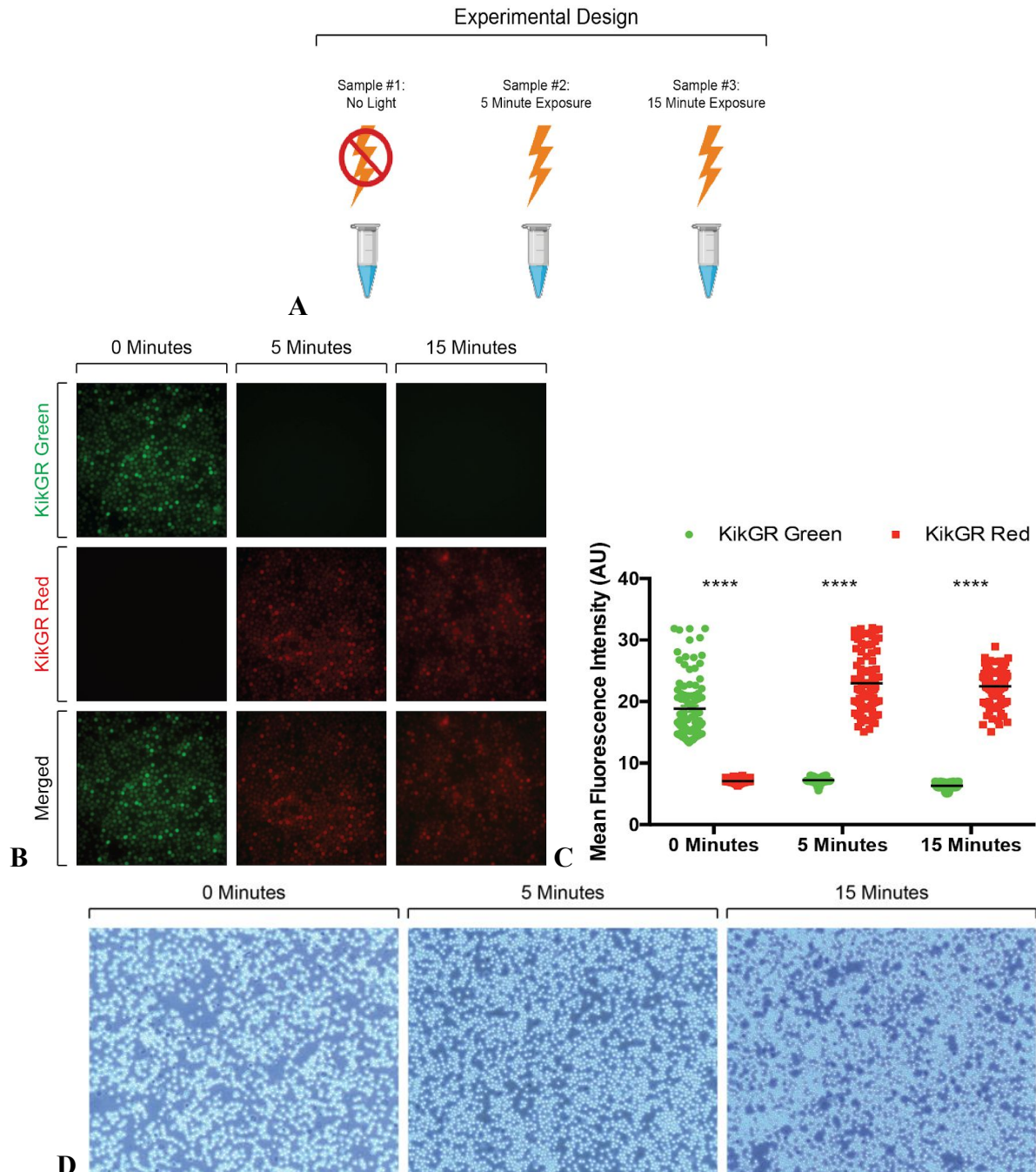


Figure 19: *A-C*, Photoconversion of KikGR cells by 405 nm LED. The average mean fluorescence intensity in arbitrary units (AU) of 100 cells were measured using ImageJ, and quantified using Graphpad Prism. Two-way ANOVA, mean \pm s.e.m., $n = 100$ cells per group, **** $p < 0.0001$. No significant differences between 5 minute/15 minute groups. **D**, Cell viability, assessed with trypan blue, showed the LED had no immediate impact on cell viability.

X. Discussion

Based on the testing conducted, the development of the device gives promising results. The spectrums measured by spectrometer of both LEDs show stable peak of the light and light intensity that meets our specifications. From our testing, the light intensity of the 405 nm LED showed that it is sufficient to photoconvert the KikGR33 mouse cells. For the 480 nm mice model LED selection, the peak wavelength is at 465.2 nm and further *in vitro* testing may be needed for evaluating its photoactivation efficacy. For the future development of the device, the LED for 480nm mice model (Ai32) may be changed to a LED with peak wavelength closer to 480 nm.

The temperature testing result shows that the temperature of the device remains in a stable range while operating and further testing is needed to test whether the device changes the mice systemic temperature by less than 1°C as specified by AAMI [7]. The 405 nm LED temperature plot, even though rises up in the first two readings, fluctuates with less than 0.5 °C range. The temperature testing is a rough approximation of the temperature change *in vivo*, and could not be interpreted as how the temperature of the device would change *in vivo*. More refined testing would need to be done before moving into *in vivo* testing of the photoconverting or photoactivating performance of the device.

The *in vitro* testing results showed the proof of concept that 405 nm LED can photoconvert most of the KikGR33 mouse cells in 5 minutes. Furthermore, the testing result also showed that there was no significant difference in the number of cells photoconverted with 5 minutes of exposure to light and 15 minutes of exposure. This information could be useful for the future testing reference point. The testing scheme may not be equivalent to *in vivo* testing, since the influences of the tissues to the light is not modeled, but the results provided information for the reference point in the future development. The *in vitro* testing for 480 nm cells was not conducted because Ai32 cells were not available for testing.

The integration of LEDs to PCB was not successful due to the limitation of the size and the spacing of the footprints. However, soldering the 480nm LEDs and soldering two 405 nm lights to a breakout board was successful and used for testing. The next improved design would take soldering limitation into consideration and space the pads on the PCB slightly farther apart and designed to be larger. For the next design iteration, the team would also 3D print or order a plastic stencil to help apply solder paste to the pads. The biomaterials researched was not coated on the LEDs, but it would be the starting point for the 405 nm LED design of future developments. The client has all IRB approval for animal testing, and they will be implanting the device so that there would be no ethical problems for applying the design to the research. Our device fills the gap between immunology and the optogenetics for its wide area of light emittance, so the application of the device would be to aid research requiring large area coverage of light.

XI. Conclusions

Tuberculosis is a serious malignancy affecting populations worldwide. Our goal is to design an implant that will allow Dr. Sandor and his lab to investigate the immune microenvironment of tuberculosis granulomas to identify potential therapeutic targets. Our final design for an implantable LED device consists of a designed PCB for the 480 nm LEDs with power connected in parallel and the data pins connected in series. The 480 nm and 405 nm LEDs will be consolidated on an improved PCB next semester. Both the 405 nm LED and 480 nm LED design will ideally be encapsulated in Parylene C in the future as it is the gold standard for coating implantable electronic devices [9]. Testing results indicated both 405 nm and 480 nm LED designs met the optimal wavelength and intensity specifications and remained at a safe temperature to be implanted in mice in future experiments. The 405 nm LED design was tested *in vitro* and effectively photoconverted KikGR cells.

Future work includes improving the PCB fabrication to allow easier soldering of the LEDs to the surface. Further testing of 480 nm LED design to photoactivate the cells also need to be done. Based on the results, our team may purchase alternative LEDs with peak wavelength close to 480 nm since the spectrum of 480 nm LED design overlaps the photo activation range of Ai32 cells but not exact. In addition to LED fabrication improvements and additional testing, we would like to incorporate a graphical user interface (GUI) for the code so that the Sandor Lab members can easily change wavelength, brightness, and pulse width modulation for the 480 nm LEDs. The GUI will help to simplify the code for users non-familiar with coding language and prevent novices from accessing the code and introducing errors/bugs.

Finally, after initial *in vivo* testing with PDMS, the electronics will be coated with Parylene C after which *in vivo* testing would be done. The adjustment of the brightness of the LED may also be made for optimizing tissue penetration once studies move *in vivo*.

XII. References

- [1] "Global tuberculosis report 2018," World Health Organization, 11-Sep-2019. [Online]. Available: https://www.who.int/tb/publications/global_report/en/. [Accessed: 08-Oct-2019]. <https://www.nationalgeographic.org/encyclopedia/bioluminescence/>. [Accessed: 10-Oct-2018].
- [2] S. A. Marcus, M. Herbath, Z. Fabry, and M. Sandor, "Dynamic changes in Mycobacterium tuberculosis-induced granulomas: developing new tools," *The Journal of Immunology*, 01-May-2018. [Online]. Available: https://www.jimmunol.org/content/200/1_Supplement/117.19. [Accessed: 08-Oct-2019].
- [3] C. Bussi and M. G. Gutierrez, "Mycobacterium tuberculosis infection of host cells in space and time," *FEMS microbiology reviews*, 01-Jul-2019. [Online]. Available: <https://www.ncbi.nlm.nih.gov/pmc/articles/PMC6606852/>. [Accessed: 08-Oct-2019].
- [4] "STOCK Tg(CAG-KikGR)33Hadj/J Overview," 013753 - STOCK Tg(CAG-KikGR)33Hadj/J. [Online]. Available: <https://www.jax.org/strain/013753>. [Accessed: 08-Oct-2019].
- [5] M. Tomura, A. Hata, S. Matsuoka, F. H. W. Shand, Y. Nakanishi, R. Ikebuchi, S. Ueha, H. Tsutsui, K. Inaba, K. Matsushima, A. Miyawaki, K. Kabashima, T. Watanabe, O. Kanagawa, "Tracking and quantification of dendritic cell migration and antigen trafficking between the skin and lymph node," *Scientific Reports*, vol. 4, no. 6030, Aug. 2014. [Online] Available: <https://www.ncbi.nlm.nih.gov/pmc/articles/PMC4129424/>
- [6] M. Tomura, N. Yoshida, J. Tanaka, S. Karasawa, Y. Miwa, A. Miyawaki, O. Kanagawa, "Monitoring cellular movement in vivo with photoconvertible fluorescence protein "Kaede" transgenic mice," *Proceedings of the National Academy of Sciences of the United States of America*, vol. 105, no. 31, pp. 10871-10876. [Online]. Available: <https://www.ncbi.nlm.nih.gov/pmc/articles/PMC2504797/>
- [7] Reichert, W. (2008). *Indwelling Neural Implants: Strategies for Contending With the in Vivo Environment (Frontiers in neuroengineering)*. CRC Press, Chapter 3.
- [8] J. Heisterkamp, R. van Hillegersberg, J.N. Ijzerman. (1999). Critical temperature and heating time for coagulation damage: implications for interstitial laser coagulation (ILC) of tumors. *Lasers in Surgery and Medicine*. Available at: <https://www.ncbi.nlm.nih.gov/pubmed/10495303>
- [9] S. Hornm "Silicone Conformal Coating vs. Parylene," *Diamond-MT, Conformal Coating*, August. 7, 2015. [Online]. Available: <https://blog.paryleneconformalcoating.com/silicone-conformal-coating-vs-parylene>. [Accessed: December 9, 2019].

- [10] S. Ahn, J. Jeong, S. J. Kim, "Emerging Encapsulation Technologies for Long-Term Reliability of Microfabricated Implantable Devices," *Micromachines (Basel)*, vol. 10, no. 8, pp. 508. 2019. [Online]. Available: <https://www.ncbi.nlm.nih.gov/pmc/articles/PMC6723304/>
- [11] Specialty Coating Systems (2007) "Parylene Properties," Specialty Coating Systems. [Online] Available: <https://www.physics.rutgers.edu/~podzorov/parylene%20properties.pdf>. [Accessed: December 10, 2019].
- [12] D. S. Lee, S. J. Kim, E. B. Kwon, C. W. Park, S. M. Jun, B. Choi, S. W. Kim, "Comparison of in vivo biocompatibilities between parylene-C and polydimethylsioxane for implantable microelectronic devices," *Bulletin of Materials Science*, vol. 36, no. 6, pp. 1127-1132. [Online]. Available: <https://www.ias.ac.in/article/fulltext/boms/036/06/1127-1132>
- [13] M. Tomura, T. Honda, K. Tanizaki, A. Otsuka, G. Egawa, Y. Tokura, H. Waldmann, S. Hori, J. G. Cyster, T. Watanabe, Y. Miyachi, O. Kanagawa, K. Kabashima, "Activated regulatory T cells are the major T cell type emigrating from the skin during a cutaneous immune response in mice," *The Journal of Clinical Investigation*, vol. 120, no. 3, pp. 883-893. [Online]. Available: <https://www.ncbi.nlm.nih.gov/pmc/articles/PMC2827959/>
- [14] A. Prabhakar, D. Vujovic, L. Cui, W. Olson, W. Luo, B. Arenkiel, "Leaky expression of channelrhodopsin-2 (ChR2) in Ai32 mouse lines," *PLOS One*, vol. 14, no. 3. [Online]. Available: <https://www.ncbi.nlm.nih.gov/pmc/articles/PMC6435231/>
- [15] L. Madisen, T. Mao, H. Koch, J. Zhuo, A. Berenyi, S. Fujisawa, Y. A. Hsu, A. J. Garcia III, X. Gu, S. Zanella, J. Kidney, H. Gu, Y. Mao, B. M. Hooks, E. D. Boyden, G. Buzsaki, J. M. Ramirez, A. R. Jones, K. Svoboda, X. Han, E. E. Turner, H. Zeng, "A toolbox of Cre-dependent optogenetic transgenic mice for light-induced activation and silencing," *Nature Neuroscience*, vol. 15, no. 5, pp. 793-802. [Online]. Available: <https://www.ncbi.nlm.nih.gov/pmc/articles/PMC3337962/>
- [16] USHIO, Deep UV Lamp Spot-Cure Series - Spot UV Curing Equipment, Tokyo Instruments, 2019. Accessed on: December. 9, 2019. [Online]. Available: <http://www.tokyoinst.co.jp/en/products/detail/UD02/index.html>
- [17] Blue Sky Research, Fiber Coupled Lasers, Blue Sky Research, 2019. Accessed on: December. 9, 2019. [Online]. Available: <https://blueskyresearch.com/products/fiber-coupled-lasers-and-systems/fiber-coupled-lasers/>
- [18] Y. Chen, Y. Kim, B. Tillman, W. Yeo, Y. Chun, "Advances in Materials for Recent Low-Profile Implantable Bioelectronics," *Materials (Basel)*, vol. 11, no. 4, pp. 522. [Online]. Available: <https://www.ncbi.nlm.nih.gov/pmc/articles/PMC5951368/>
- [19] Kim, S.H., Moon, J.H., Kim, J.H. et al. *Biomed. Eng. Lett.* (2011) 1: 199. <https://doi.org/10.1007/s13534-011-0033-8>

- [20] Chen P.-J., Rodger D.C., Agrawal R., Saati S., Meng E., Varma R., Humayun M.S., Tai Y.-C. Implantable micromechanical parylene-based pressure sensors for unpowered intraocular pressure sensing. *J. Micromech. Microeng.* 2007;17:1931. doi: 10.1088/0960-1317/17/10/002.
- [21] Kuo J.T., Kim B.J., Hara S.A., Lee C.D., Gutierrez C.A., Hoang T.Q., Meng E. Novel flexible parylene neural probe with 3d sheath structure for enhancing tissue integration. *Lab Chip.* 2013;13:554–561. doi: 10.1039/C2LC40935F.
- [22] Massachusetts Institute of Technology, "Material: PDMS (polydimethylsiloxane)," Massachusetts Institute of Technology. [Online]. Available: <http://www.mit.edu/~6.777/matprops/pdms.htm>. [Accessed: December 10, 2019].
- [23] H. Zhao, "Recent Progress of Development of Optogenetic Implantable Neural Probes," *International Journal of Molecular Sciences*, vol. 18, no. 8, p. 1751, Nov. 2017.
- [24] AzoMaterials, "MasterSil 151 Med:Silicone Compound for Medical Applications," MasterSil, 2019. [Online]. Available: <https://www.azom.com/equipment-details.aspx?EquipID=6296>. [Accessed: December 10, 2019].
- [25] Aquilina K., Thoresen M., Chakkarapani E., Pople I.K., Coakham H.B., Edwards R.J. Preliminary evaluation of a novel intraparenchymal capacitive intracranial pressure monitor. *J. Neurosurg.* 2011;115:561–569. doi: 10.3171/2011.4.JNS101920.
- [26] L.L. Moen, "An Implantable Device for Nerve Stimulation," M.S. thesis, Department of Engineering Cybernetics, Norwegian University of Science and Technology, July 2014. Accessed on: 8-Oct-2019. [PDF]. Available: <https://pdfs.semanticscholar.org/4e54/0c5767d9fd18e868a6f54acfe4bab8cb9b87.pdf>
- [27] Vishay Semiconductors, "UV SMD LED PLCC-2," VLMU3100 datasheet, 26-June-2017. Accessed on: 8-Oct-2019.
- [28] Szledcolor, "SK6812 SPECIFICATION INTEGRATED LIGHT SOURCE INTELLIGENT CONTROL OF CHIP-ON-TOP SMD TYPE LED," SK6812 Datasheet, 25-April-2016. Accessed on: 8-Oct-2019.
- [29] V&P Scientific, Inc., "Parylene Properties and Characteristics," 2010. [Online]. Available: http://www.vp-scientific.com/parylene_properties.htm. [Accessed: December 10, 2019].
- [30] Adafruit. (2019, December. 9). 5050 LED breakout PCB - 10 pack! [Online]. Available: <https://www.adafruit.com/product/1762>
- [31] Fabry, Z., Chreiber, HS., Harris, MG., Sandor, M. (2008). Sensing the microenvironment of the central nervous system: immune cells in the central nervous system and their

pharmacological manipulation. *Curr Opin Pharm.* doi: 10.1016/j.coph.2008.07.009.

[32] The Staff of the Jackson Laboratory. *Biology of the Laboratory Mouse*. New York: *Dover Publications INC.*, 1966.

[33] Bonin, R. P., Wang, F., Desrochers-Couture, M., Gassecka, A., Boulanger, M., Côté, D. C., & Koninck, Y. D. (2016). Epidural optogenetics for controlled analgesia. *Molecular Pain*, *12*, 174480691662905. doi:10.1177/1744806916629051

[34] Towne, C., Montgomery, K. L., Iyer, S. M., Deisseroth, K., & Delp, S. L. (2013). Optogenetic Control of Targeted Peripheral Axons in Freely Moving Animals. *PLoS ONE*, *8*(8). doi:10.1371/journal.pone.0072691

Appendix I: Product Design Specification (PDS)

Function:

The discovery of microbial opsin genes, which is a group of genes that was first studied in neurons, makes it possible to selectively control activation or silencing of neurons or other cells by light. Optogenetics is the study that combines optics with tissue genetically modified to express light-sensitive channels in the cell membrane. Our client aims to study immune trafficking in tuberculosis and inflammation of the brain by using optogenetics [31]. Our group's product will be safe to be implanted in mice and should emit light within certain wavelength requirement. The light source can also be switched on and off easily by operator for research use. The light's intensity is able to trigger all of the light sensitive channels inside the mouse tissue.

Client requirements:

The goal of our client is to use optogenetic activation or blocking of neurons to alter immune cell functions in mice to understand inflammatory responses in brain and lung diseases [31]. In vivo light delivery is key to this project and our client needs a solution for 480nm and possible 405nm light that can deliver light to a larger area, which is about one square centimeter, and can be switched on and off for specific increments in the mice. The heat produced by the light should neither be harmful nor kill the cells and tissues near implantation site. The light should be delivered deep enough to stimulate the lung tissue of the mice without causing harmful phototoxicity. The light should also be reusable if it is expensive to fabricate.

Design requirements:

1. Physical and Operational Characteristics

a. Performance requirements:

The device will be turned on for the complete duration of the experiment which will last for two hours. Not only does the device need to be powered for the duration of the experiment, it must continue to be functional and biocompatible under physiological conditions within the mouse's subcutaneous tissue (wet, temp: 36.9 °C, pH: 6-8) [32].

Light must have a size of approximately one square centimeter with a broad light source range able to penetrate deep into the organs of the mice. It also needs to have a wavelength of 405nm and/or 480nm without producing UV rays that may damage the tissue.

Light source must be able to be switched on and off for 15-30 second intervals over each 2-hour experiment. The light source must be flexible and able to be inserted subcutaneously to the mice's skull.

b. Safety:

The heat generated by light should be minimal and not be harmful to neighboring cells and tissues. The thermal tolerance for implantable devices is approximately 1 °C. During the duration of the experiment, the device should be able to diffuse the heat from the light emitting diode to prevent thermal damage. In addition, the team should make sure the UV light is not produced by the light source as the UV light would cause harm to the cells. The device should also be designed to limit phototoxicity of the living tissue. The material should also be biocompatible so that it will not cause an inflammatory response in the tissue. Electronic components of the device will be coated in a biocompatible and implantable material (example parylene C or PDMS) to prevent voltages and currents from harming the mice.

c. Accuracy and Reliability:

The light needs to be durable and biocompatible so that it is able to withstand the environment inside the blood vessels of mice. Also, the light source developed should be broad enough to cover enough areas on the organs of the mice to make sure the light-sensitive genes can be triggered and monitored. The light emitting diodes should emit wavelengths of 405nm and 480nm.

d. Life in Service:

Ideally the electrical components of the device will be reusable while the coating biomaterial would be covering the light and could be sterilized by ethanol. The light source should also work continuously and consistently without unpredicted damage in the hardware. The heat sink would also aid performance in maintaining the energy from dissipating in the form of heat to maintain light intensity for the time during use.

e. Operating Environment:

The device will be exposed to physiological conditions in the subcutaneous tissue of the mice in the chest and cranium. The device will be exposed to the body temperature and pH of the mice which is approximately 36.9 °C and pH 6-7, respectively [32]. Since the device is in an aqueous, saline environment, there is risk of corrosion and/or electric shock. The individuals at risk are the mouse itself or the person carrying out the experiment and this risk must be mitigated.

f. Ergonomics:

The device should be readily and easily picked up using tweezers. Once the device is in the mouse, it will not be handled by a human until it needs to be removed - a microcontroller will simply need to be turned on to operate the device.

g. Aesthetics, Appearance, and Finish:

The design needs to be small, compact, and streamlined. Since the design will be used *in vivo*, wires are acceptable but not preferred. The materials used need to be durable and able to function when in the subcutaneous environment of the mice. The device needs to be biocompatible and prevent any form of liquid from seeping into the device.

2. Production Characteristics

a. Target Product Cost:

The client did not specify the budget as long as we make reasonable use of the money provided by our client. Our team will try to minimize the amount we might spend and try to make our device reusable and reliable.

3. Miscellaneous

a. Standards and Specifications: FDA Regulation of Implantable Medical Devices

Our device to be built will be implanted subcutaneously in the mouse. According to the FDA the ambient temperature must not increase by more than 1°C or brain damage may occur [7].

b. Customer:

For a preliminary design specification in regard to customer, the device should be user-friendly (easy to handle, will not fall apart easily when mishandled, etc). This device will not be available to the commercial consumer - it will be used for research purposes at the client's research lab.

c. Patient-related concerns:

Our design will not be applied to patients directly even though the ultimate goal might be to alter immune response of humans. For our research subjects, mice, the use of light source must not be detrimental to the research projects and the device should be safe to mice when being implanted.

d. Competition:

1. Biocompatible optical fiber-based nerve cuff can be used for light delivery that wraps around the target neuron. The research mainly considers light delivery to peripheral axons [33].
2. Epidural fiber-optic implants:
Epidural fiber is used in light delivery for spinal cords. The system [34] enables sufficient light intensity and different light wavelength to be delivered.

NOTE: References of PDS have been added to references of this final report.

Appendix II: Testing Result Calculation

Table 3: Maximum light intensity (mW/cm^2) in the two experiments. This testing was from the previous semester.

	480 nm Peak Strength average(mW/cm^2)	520nm Peak Strength average(mW/cm^2)
No PDMS	774.5796 (oversaturated)	225.9
With PDMS	774.5796 (oversaturated)	646.6

Appendix III: Material Costs

Table 4: Fall 2019 Design Project Expenses

Material	Quantity	Cost
Printed Circuit Board (PCB)	10	\$43.00
DotStar 5050 RGB LED	20	\$47.10
5050 LED Breakout PCB	10	\$15.97
Microcontroller and Circuitries	N/A	\$0.00
Ocean Optics Spectrometer	1	\$0.00
	Total	\$106.07

Appendix IV: Arduino Code

```
// ledmau5 NodeMCU ESP8266 Microcontroller driver
```

```
#include <Adafruit_NeoPixel.h> //access Neopixel library to communicate to LEDs
```

```
#include <Ticker.h>
```



```

class LEDStrip {
private:
    static const int NUMPIXELS = 4; // Number of NeoPixels on the board
    int period = 0; // Regular interval or period of cycle
    int cyc_cnt = 0; // Number of cycles since flash start
    long int cyc_max = 0; // Number of on/off cycles to complete
    int rgb[3]; // RGB color of LED's [r, g, b]
    int brightness = 0; // LED brightness index
    float dcyc = 0; // Duty cycle or proportion of period where pixels are on
    bool is_on = false; // status of LED illumination, default off
    Adafruit_NeoPixel* pixels; // NeoPixel controller object
    Ticker period_ticker; // Timer to trigger beginning of period/duty cycle
    Ticker dcyc_ticker; // Timer to trigger end of duty cycle within period

    void duty_on() {
        this->dcyc_ticker.attach_ms(round(this->period * this->dcyc),
std::bind(&LEDStrip::duty_off, this));
        this->pix_on();
    }

    void duty_off() {
        this->dcyc_ticker.detach();
        if (++this->cyc_cnt >= this->cyc_max) { // exposure finished
            this->period_ticker.detach();
        }
        this->pix_off();
    }

public:
    LEDStrip(int pin) {
        // When setting up the NeoPixel library, we tell it how many pixels,
        // and which pin to use to send signals. Note that for older NeoPixel
        // strips you might need to change the third parameter -- see the
        // strandtest example for more information on possible values.
        this->pixels = new Adafruit_NeoPixel(LEDStrip::NUMPIXELS, pin, NEO_GRB +
NEO_KHZ800);
        this->pixels->begin(); // INITIALIZE NeoPixel strip object (REQUIRED)
    }
}

```

```

void pix_off() {
    this->pixels->clear();
    this->pixels->show();
    this->is_on = false;
}

void pix_on() {
    this->pixels->fill(this->pixels->Color(
        this->rgb[0], // red value
        this->rgb[1], // blue value
        this->rgb[2] // green value
    )
    );
    this->pixels->setBrightness(this->brightness);
    this->pixels->show();
    this->is_on = true;
}

void start_flash(int period, float dcyc, long int cyc_max) {
    this->period_ticker.detach();
    this->dcyc_ticker.detach();
    this->period = period;
    this->dcyc = dcyc;
    this->cyc_max = cyc_max;
    this->cyc_cnt = 0;
    if (cyc_max < 0) {
        this->pix_on();
    } else if (round(this->period * this->dcyc) == this->period) { // solid light, no flash, 100%
duty cycle
        this->pix_on();
        this->period_ticker.attach_ms(this->period * this->cyc_max, std::bind(&LEDStrip::pix_off,
this));
    } else {
        this->duty_on();
        this->period_ticker.attach_ms(this->period, std::bind(&LEDStrip::duty_on, this));
    }
}

// convert wavelength (nm) to an rgb value stored in a three member

```

```

// array for each color index i.e. [0=r, 1=g, 2=b]
void set_color(int wl) {
    float wavelength = (float)wl;
    float gamma = 0.8;
    float attenuation = 0.0;
    int* rgb = new int[3];
    float r, g, b;
    r = g = b = 0.0;
    if (wavelength >= 380 && wavelength <= 440) {
        attenuation = 0.3 + 0.7 * (wavelength - 380) / (440 - 380);
        r = pow(((1 - (wavelength - 440)) / (440 - 380)) * attenuation, gamma);
        g = 0.0;
        b = pow((1.0 * attenuation), gamma);
    } else if (wavelength >= 440 && wavelength <= 490) {
        r = 0.0;
        g = pow((wavelength - 440) / (490 - 440), gamma);
        b = 1.0;
    } else if (wavelength >= 490 && wavelength <= 510) {
        r = 0.0;
        g = 1.0;
        b = pow((-1 * (wavelength - 510)) / (510 - 490), gamma);
    } else if (wavelength >= 510 && wavelength <= 580) {
        r = pow(((wavelength - 510) / (580 - 510)), gamma);
        g = 1.0;
        b = 0.0;
    } else if (wavelength >= 580 && wavelength <= 645) {
        r = 1.0;
        g = pow((-1 * (wavelength - 645)) / (645 - 580), gamma);
        b = 0.0;
    } else if (wavelength >= 645 && wavelength <= 750) {
        attenuation = 0.3 + 0.7 * (750 - wavelength) / (750 - 645);
        r = pow((1.0 * attenuation), gamma);
        g = 0.0;
        b = 0.0;
    } else {
        r = 0.0;
        g = 0.0;
        b = 0.0;
    }
}

```

```

this->rgb[0] = (int)(r * 255);
this->rgb[1] = (int)(g * 255);
this->rgb[2] = (int)(b * 255);

if (this->is_on) {
    this->pix_on(); // refresh with new color
}
}

void set_brightness(int b) {
    this->brightness = b;
    if (this->is_on) {
        this->pix_on(); // refresh with new brightness
    }
}
};

LEDStrip* strips[9]; // NodeMCU can control up to 9 mice LED strips
#define BUF_SIZE 64
char _buffer[BUF_SIZE];
int buf_idx = 0;

void run_cmd() {
    int pix_dpin = atoi(strtok(_buffer, "/"));
    char* func = strtok(strtok(NULL, "/"), "?");
    char* f_args = strtok(NULL, "?");

    if (*func == 'c') { // change pixel color
        strips[pix_dpin]->set_color(atoi(f_args));
    }
    if (*func == 'b') { // change pixel brightness
        strips[pix_dpin]->set_brightness(atoi(f_args));
    }
    if (*func == 'f') { // start flash exposure
        int period = atoi(strtok(f_args, ":"));
        float dcyc = atof(strtok(NULL, ":"));
        int cyc_max = atol(strtok(NULL, ":"));
        strips[pix_dpin]->start_flash(period, dcyc, cyc_max);
    }
}

```

```

}

// reset read-in buffer
buf_idx = 0;
_buffer[0] = 0;
}

void receive_byte(int byte_read) {
  if (buf_idx == BUF_SIZE - 1) buf_idx = 0;
  if (byte_read == '[') { // begin reading command
    buf_idx = 0;
  } else if (byte_read == ']') { // start processing command
    run_cmd();
  } else { // write out character to buffer
    _buffer[buf_idx++] = byte_read;
    _buffer[buf_idx] = 0;
  }
}

void setup() {
  Serial.begin(115200);
  // create all LED strip objects and map to NodeMCU GPIO pin
  //strips[0] = new LEDStrip(16); // D0 cannot be setup, needs further debugging
  strips[1] = new LEDStrip(5); // D1
  strips[2] = new LEDStrip(4); // D2
  strips[3] = new LEDStrip(0); // D3
  //strips[4] = new LEDStrip(2); // D4 needs to be pulled down, starts high
  strips[5] = new LEDStrip(14); // D5
  strips[6] = new LEDStrip(12); // D6
  strips[7] = new LEDStrip(13); // D7
  strips[8] = new LEDStrip(15); // D8
}

void loop() {
  if (Serial.available() > 0) {
    receive_byte(Serial.read());
  }
}

```

[<pix_index>/c?<wavelength(nm)>]

[<pix_index>/b?<brightness>]

[<pix_index>/f?<period(ms)>:<duty_cycle>:<cycles>]

Figure 20. The format of the command input for Arduino.

Appendix V: MATLAB Code

```
file = uigetfile('.txt'); // tell Matlab to access the txt file
A = load(file); // load txt file into the variable A
reference = [470.2540,470.6100];
wavelength = A(400:1400,1);
counts = A(400:1400,2);
Light_Energy = zeros(size(wavelength,1),1);

for i = 1:size(wavelength,1)
    Light_Energy(i,:) = counts(i,:) * 10 * 3e8 * 6.63e-34*1e9/(wavelength(i,:));
end
intensity = 1000*Light_Energy*10000/(0.025^2*2048*14e-6*200e-6) // conversion of counts to
figure; // intensity
p = plot(wavelength,intensity,'b-','LineWidth',2);
ylabel('Light Intensity (mW/cm^2)');
xlabel('Wavelength(nm)');
title('Intensity vs. Wavelength');
```